Influence of Water Stability on Bond Performance Between Magnesium Phosphate Cement Mortar and Steel Fibre

Hu Feng[1], Guanghui Liu[1], Jiansong Yuan[2, *], M. Neaz Sheikh[3], Lu Feng[4] and Jun Zhao[1]

Abstract: The fibre pullout test was conducted to investigate the influence of the water stability on the bond behaviour between the Magnesium phosphate cement (MPC) matrix and the steel fibre. The composition of the MPC-matrix and the immersion age of the specimens are experimentally investigated. The average bond strength and the pullout energy are investigated by analysing the experimental results. In addition, the microscopic characteristics of the interface transition zone are investigated using scanning electron microscopy (SEM). The experimental results showed that the bond performance between the MPC-matrix and the steel fibre decreased significantly with the increase of the duration of immersion in water. The average bond strength between the steel fibre and the MPC-matrix reduced by more than 50% when the specimens were immersed in the water for 28 days. The effect of the water on the interface between the steel fibre and the MPC-matrix was found to be more significant compared to the composition of the MPC-matrix. In addition, the MgO-KH$_2$PO$_4$ mole ratio of the MPC significantly influenced the water stability of the interface zone between the steel fibre and MPC-matrix.

Key words: Steel fibre, pullout, water stability, magnesium phosphate cement, bond behaviour.

1 Introduction

Magnesium phosphate cement (MPC) is a new type of inorganic cementing material mainly made from over-burning magnesia and phosphate [Meng, Deng and Sun (2014)]. In comparison with the ordinary Portland cement, the MPC possesses excellent properties including (1) rapid gain of strength and condensation; (2) higher early strength (the compressive strength can reach 20 MPa within 1 hour and 40 MPa within 3 hours); (3) ability to solidify and harden at low temperatures (as low as -20°C); (4) excellent bonding strength; (5) high durability (including chemical resistance, frost resistance and permeability). Existing studies [Yan (2010); Yang, Zhu and Wu (2000); Ding (2005);

[1] School of Civil Engineering, Zhengzhou University, Zhengzhou, 450001, China.

[2] School of Civil Engineering, Henan University of Engineering, Henan, 451191, China.

[3] School of Civil, Mining and Environmental Engineering, University of Wollongong, NSW 2522, Australia.

[4] Yellow River Engineering Consulting Co., Ltd., Henan, 450003, China.

[*] Corresponding Author: Jiansong Yuan. Email: yuanjiansong@hotmail.com.

Xiao (2015)] show that the MPC has good compatibility with the ordinary Portland cement and has excellent bonding properties to meet the requirements of the repairing materials. The bond strength between the MPC and existing concrete has been found to be sufficient, especially at the early bond strength [Yang and Wu (1999)]. The use of MPC paste as an interface agent can improve the bond strength [Yang (2014)]. Therefore, the MPC has been widely used in repairing existing construction and quick-construction in recent years, such as concrete pavements, bridge decks and airstrips.

The MPC is a brittle material like the Portland cement-based material. The brittleness increases as the strength of the MPC increases. It is necessary to incorporate fibres into the matrix to increase the plasticity and toughness. Existing studies have demonstrated the feasibility of using MPC to prepare the fibre reinforced composites [Frantzis and Baggott (2000); Frantzis and Baggott (2003)]. Incorporating suitable type and dosage of fibres can significantly improve the brittleness of the MPC matrix. The reinforcing effect of steel fibre on the MPC based composite is greater than the reinforcing effect of steel fibre on the Portland based composites [Feng, Sheikh, Hadi et al. (2018)]. After immersed in hot water of 60°C and subjected to the dry and wet cycles, the ordinary silicate-based composites become more brittle, while the strength and toughness of the polypropylene and steel fibre reinforced MPC composites are well maintained [Pera and Ambroise (1998)]. The shrinkage of the MPC mortar was reduced significantly by incorporating steel fibres [Wang, Qian, Cao et al. (2006)]. Also, several studies have shown that steel fibres could be used to improve the flexural strength, tensile strength, flexural toughness, and adhesion to concrete compared to chemical fibres and the natural fibres [Yang and Wu (1999)]. For example, the MPC reinforced by steel fibre could significantly improve the compressive strength, flexural strength, flexural toughness and flexural ductility of MPC matrix composites [Feng, Chen, Gao et al. (2018)]. Zhao [Zhao (2017)] reported that steel fibres with 0.8%-1.6% by volume prevented cracks of the MPC concrete. The improvement effect of the steel fibre reinforced MPC depends largely on the bond behaviour between the fibre and MPC. Therefore, the interfacial bond behaviour influences significantly the performance of the steel fibre reinforced MPC. The physicochemical bond between the steel fibre and the matrix prepared with MPC is much better than the physicochemical bond between the steel fibre and the matrices prepared with Portland cement [Feng, Sheikh, Hadi et al. (2018)]. The fibre pullout tests are commonly used to test interfacial adhesion between the fibres and the substrates [Shanng, Brincker and Hansen (1999)]. However, when the MPC is used in some projects located in a humid or rainy environment, the durability of the MPC may not be ensured. The influence of the water on the bond behaviour between the steel fibre and MPC is not known. At present, there are several research studies on the water resistance and modification of magnesium oxychloride cement [Soudée and Péra (2002)], but only a few studies were conducted on bond performance between MPC and steel fibre.

The influence of water stability on bond behaviour between MPC mortar and steel fibre was investigated experimentally in this study. A series of pullout tests of steel fibres embedded in the MPC-based matrix was carried out. The parameters investigated in this experimental study included the composition of the MPC matrix and the immersion age of the specimens. The average bond strength and pullout energy were investigated. The influence of water stability on the microscopic characteristics of the interface transition

zone was also analyzed by using scanning electron microscope (SEM).

2 Experimental program

2.1 Material

The over-burning magnesia (denoted as M) is provided by Xinmi City Zhengyang Foundry Material Factory. The specific surface area of over-burning magnesia is 325 m^2/kg. The oxide composition magnesia powder is reported in Tab. 1. The potassium dihydrogen phosphate with a KH_2PO_4 content of 98% (denoted as P) is obtained from Wujiang Weitong Chemical Co., Ltd. The borax (chemical formula: $Na_2B_4O_7 \cdot 10H_2O$, denoted as B) with a purity of 95% was obtained from Liaoning Borda Technology Co., Ltd. The calcium chloride with a purity of 96.0% was obtained from Tianjin Komiou Chemical Reagent Co., Ltd. The granular crystals were grounded into powder before specimen preparation. The disodium hydrogen phosphate dodecahydrate with a purity of 99.0% was obtained from Tianjin Komiou Chemical Reagent Co., Ltd. The crystals were screened by using 0.6 mm square hole screen before specimen preparation. The natural river sand was the medium sand and screened by the 2.36 mm standard square hole. The fineness modulus of the sand was 2.06. The steel wire cut straight fibre obtained from Shanghai Bekaert Company had a diameter of 0.75 mm.

Table 1: Oxide Composition of the magnesia powder

Oxide Composition	MgO	SiO$_2$	CaO	Fe$_2$O$_3$	Ignition loss
Content (%)	92.53	3.1	1.6	0.87	1.9

2.2 Specimen preparation and test methods

The specimen of the pullout test for steel fibre and magnesium phosphate cement (MPC) mortar was cast by using the dog-bone-shaped mould. A steel partition with a thickness of 1 mm was placed in the middle of the test mould, and four steel fibres were evenly embedded in the steel partition. The fixed end of the steel fibre was formed at first. Afterwards, the pullout end was formed. The 40 mm×40 mm×160mm prism specimens were simultaneously cast during the moulding process. The specimen is shown in Fig. 1. The specimen size is shown in Fig. 2. Tab. 2 shows the immersion time of the specimens and proportion of the matrix.

Figure 1: Dog-bone-shaped specimen

(a) Top view of the specimen   (b) Side view of the specimen   (c) Section A-A
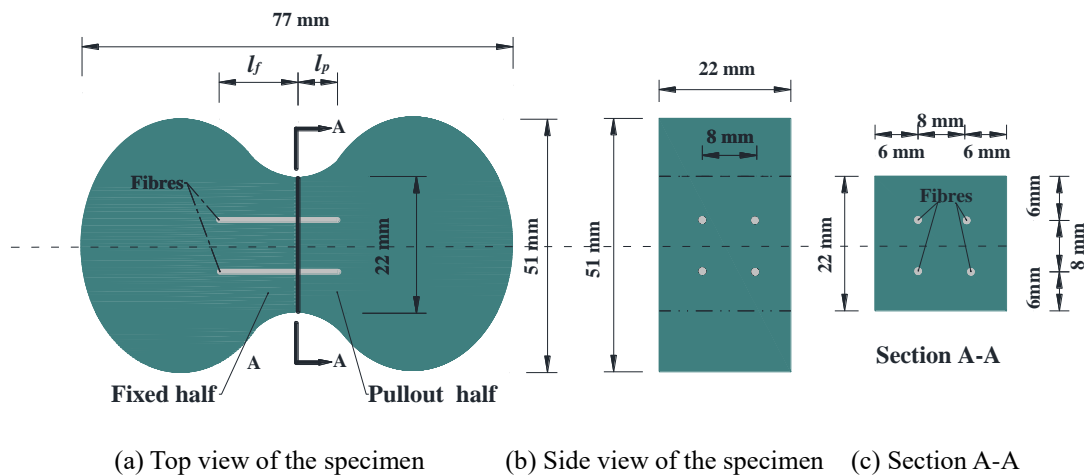
Figure 2: Illustration of the dog-bone-shaped specimen

The fixed half of the dog-bone-shaped specimen was cast according to the following steps: (1) the solid raw materials including the magnesia, retarder, potassium dihydrogen phosphate and sand were mixed evenly by a mixer at a low speed. Then water was added and mixed at a low speed for 15 s and a high speed for 50 s; (2) the fixed half was cast into the mould and then the mould was vibrated for 200 s; (3) the specimens were demolded after 2 hours.

After the fixed half of the specimen was demolded, the mould was disassembled and the partitioning board was removed. The cling wrap was used to cover the fixed half to prevent adhesion between the two halves of the specimens. Finally, the paste was cast into the other half (pullout half) of the steel mould.

Table 2: Immersion time of the specimens and Proportion of the matrix

Immersion time (d)	Curing time (d)	Weight ratio of Water to Cement (W/C)	Weight ratio of Sand to Cement (S/C)	Mole ratio of $MgO-KH_2PO_4$ (M/P)
0				
7	7	0.14	1/0.8	3
28				
0				
7	7	0.14	1/0.8	4
28				
0				
7	7	0.14	1/0.8	5
28				
0				
7	7	0.14	1/0.8	6
28				

The flexural strength and compressive strength tests were conducted according to GB/T17671-1999 [Cement mortar strength testing method (ISO) (in Chinese) (1999)]. A universal testing machine with a capacity of 300 kN was used for the flexural strength and compressive strength tests, as shown in Fig. 3. At first, the 40 mm×40 mm×160 mm prism specimens with a span length of 100 mm were loaded in the middle to measure the flexural strength. The loading rate was 50 N/s. Afterward, the two parts of the fractured prism specimen were placed on the test setup with a compression area of 40 mm×40 mm to test the compressive strength at a loading rate of 2.4 kN/s.

Figure 3: Flexural strength and compressive strength tests

Figure 4: Pullout test

The fibre pullout test was conducted according to CECS 13-2009 [Standard test methods for fiber reinforced concrete (in Chinese) (2009)], and an electronic universal testing machine with a capacity of 5 kN was employed to determine the bond strength, as shown in Fig. 4. The loading rate was 0.5 mm/min. The slip between the fibre and the matrix was measured by an extensometer clamped onto the specimen. The test data were collected by the testing machine automatically. Five specimens were tested for each series of the fibre tests. The displayed experimental results in the paper represent the calculated average curve or average value of each series based on the test results of five specimens. The displayed curves of each series were obtained by averaging the pullout load values at regular slip increments. The interface microscopic morphology of the surface of the fibre pulled out from the matrix was analyzed by using a Scanning Electron Microscope (SEM)-(Zeiss EVO HD 15).

3 Test results and discussion

3.1 Evaluation parameters

The average bond strength (τ_{av}) [Wille and Naaman (2012)] is defined as the interfacial bond strength based on the maximum pullout load and the initial embedment length, which is given by Eq. (1):

$$\tau_{av} = \frac{P_{max}}{\pi \times d_f \times l_p} \tag{1}$$

where, P_{max} is the peak load (N) of the multiple fibres pulled out; d_f is the diameter (mm) of the fibre; l_p the initial embedment length of the fibre in the pullout half of the specimen.

The total pullout energy (W_p) is defined as the energy when the slip of the fibre reach to 2.0 mm, which could be obtained by the integration of the area under the pullout load-slip curve [Gao (2014)], and is given by Eq. (2).

$$W_P = \int P(s)ds \tag{2}$$

The strength retention rate (K_m) is defined as the ratio of the strength after immersion to the strength under natural condition of curing [Gao (2014)] and is given by Eq. (3).

$$K_m = \frac{M_t}{M} \tag{3}$$

where, M_t is the compressive strength of the matrix after immersion, and M is the initial compressive strength of the MPC matrix.

3.2 Discussion

The specimens were cured under the ambient condition (approximately at a relative humidity of 55% and a temperature of 20°C) for 7 days, and then immersed in the water for 7 days and 28 days, respectively. The compressive strength and the bond behaviour of the specimens with different curing conditions were compared. The experimental results are shown in Tabs. 3 and 4.

Table 3: Compressive strength and retention rate of compressive strength at different immersion age

M/P	Immersion time (d)	Compressive strength (MPa)	Intensity retention rate (%)
3		24.9	--
4	0	37.4	--
5		37.0	--

6		30.6	--
3		21.2	85.1
4	7	35.1	93.9
5		32.5	87.8
6		27.8	90.8
3		16.8	67.5
4	28	29.7	79.4
5		29.5	79.7
6		24.9	81.4

Table 4: Bonding properties at different immersion age

M/P	Immersion time (d)	Average bond strength (MPa)	Average bond strength retention (%)	Pullout energy (N·mm)	Pullout the energy retention rate (%)
3		2.72	--	295.80	--
4	0	4.53	--	632.99	--
5		4.46	--	502.50	--
6		3.51	--	440.44	--
3		1.77	65.1	248.12	83.9
4	7	3.42	75.5	428.82	67.7
5		2.73	61.2	362.76	72.2
6		2.18	62.1	291.53	66.2
3		1.15	42.2	153.04	51.7
4	28	2.60	57.4	328.20	51.8
5		1.89	42.4	264.22	52.6
6		1.57	44.7	186.76	42.4

3.2.1 Compressive strength

The compressive strength of the specimens with different immersion age is shown in Fig. 5. It is clear that the compressive strength decreased with the increase of the immersion age. In addition, the optimum value of M/P is 4 for the compressive strength. The above-mentioned experimental results could be explained by the hydration reaction in the MPC matrix [Ding, Dong, Xing et al. (2012)], in which a kind of $MgKPO_4 \cdot 6H_2O$ (MKP) crystals is produced. The MKP crystals can overlap each other and form a skeleton structure. The magnesium oxide is filled in the middle to form a dense matrix. When the pH of the aqueous solution is larger than 7, the reaction proceeds in the positive direction, the content of MKP increases and contributes to a higher compressive strength. If the aqueous solution is acidic (pH<7), the reaction proceeds in an adversely opposite direction, and the MKP is decomposed leading to the decrease of the compressive strength.
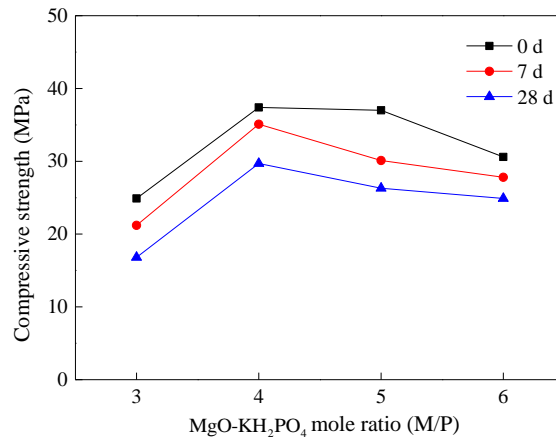
Figure 5: Compressive strength of MPC based mortar at different immersion age

After the specimen was immersed in water, the unreacted potassium dihydrogen phosphate in the matrix was dissolved leading to the acidic aqueous solution. As a result, the reaction proceeded in the opposite direction and the content of MKP is reduced. Therefore, the compressive strength was reduced. Theoretically, the more the potassium dihydrogen phosphate remaining in the matrix (i.e., the smaller the M/P), the faster the rate of matrix strength decline after immersion in water.

3.2.2 Pullout load-slip curves

The pullout load-slip curves of the specimens at different immersion ages are shown in Fig. 6. The bond behaviour was significantly affected after the specimens were immersed in the water, and the pullout load exhibited varying degrees of decline. It should be noted that the peak load decreased significantly, and the decline for the immersion time of 7 days was larger than the decline for the immersion time of 28 days. This is because the longer immersion time caused the damage of the interface and led to the weak bond strength.
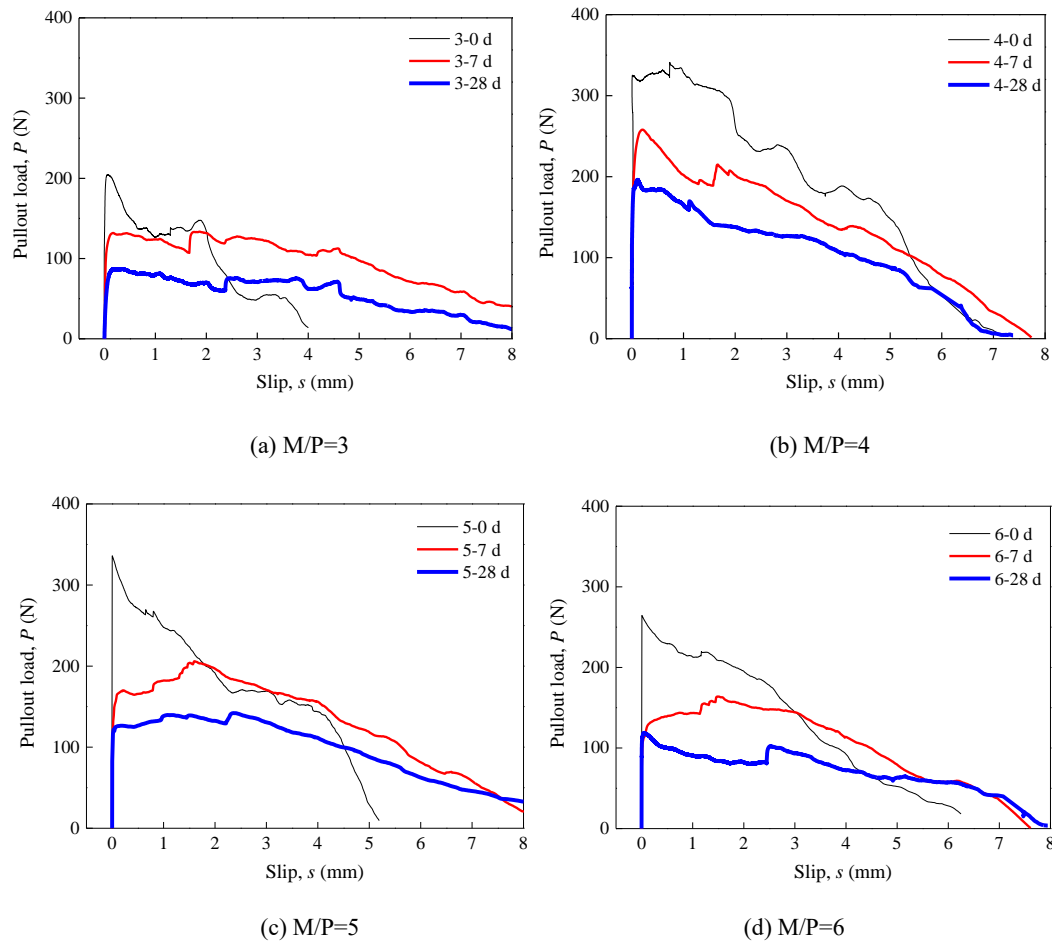
(a) M/P=3   (b) M/P=4

(c) M/P=5   (d) M/P=6

Figure 6: Pulling load-slip curve of the fibre embedded in MPC at different immersion age

The peak pullout load was affected by the M/P. The peak pullout load increased with the increase in the M/P from 3 to 4 and then decreased with the increase in M/P from 4 to 6. The maximum peak load was obtained when the M/P was 4. It is clear that the bonding performance between the matrix and the fibres were influenced significantly after the immersion in the water.

3.2.3 Bond strength and pullout energy

The bond strength versus M/P curves and the pullout energy versus M/P curves are shown in Fig. 7 and Fig. 8, respectively. The bond strength showed a similar change with the pullout load. When the M/P increased from 3 to 4, all the corresponding average bond strength was almost improved by 2 MPa. However, the average bond strength showed a decline when the M/P was larger than 4. For the specimens immersed in the water, the decline of the average bond strength was more apparent. The pullout energy versus M/P curves showed a similar change with the bond strength versus M/P curves.
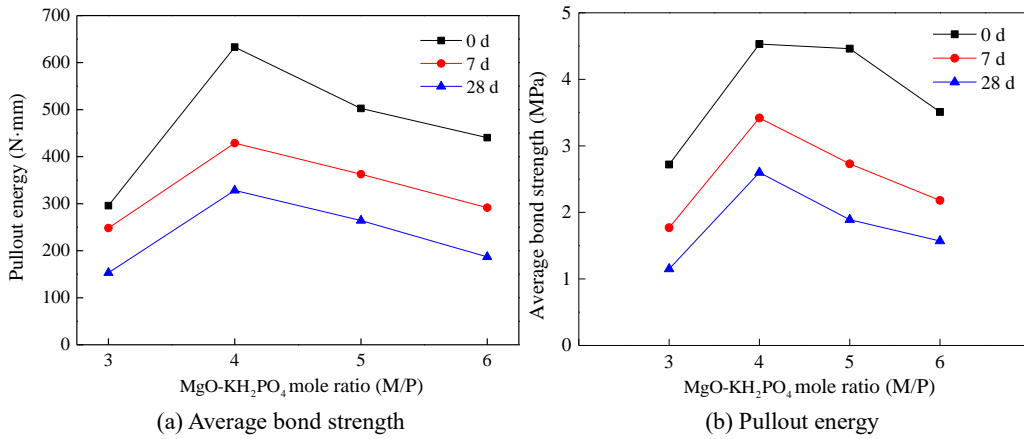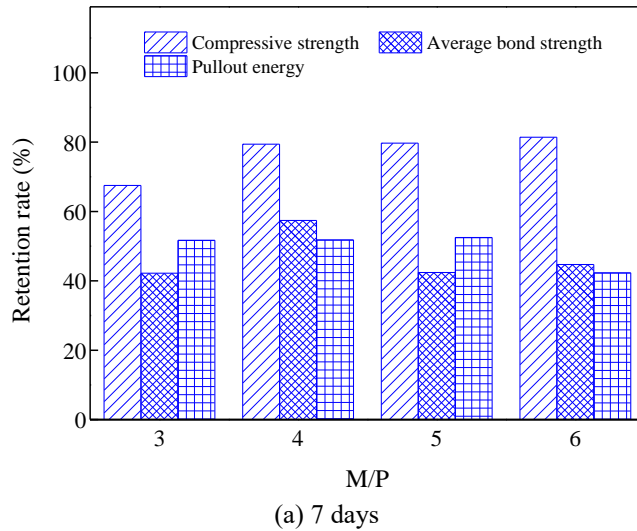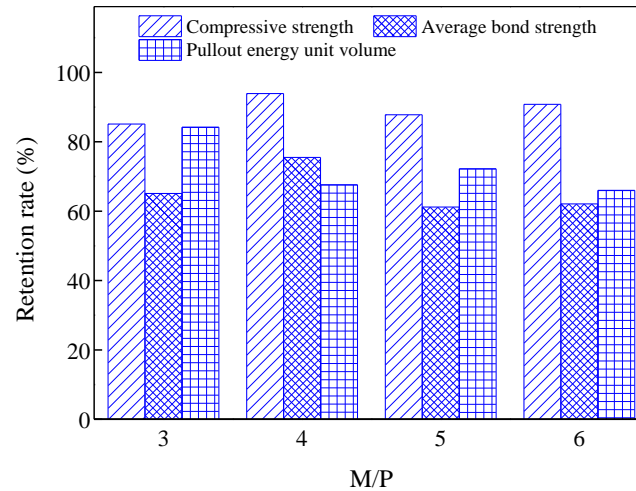
(a) Average bond strength   (b) Pullout energy

Figure 7: Bonding properties between the steel fibre and MPC matrix at different immersion age

The influence of the water on the bond strength could also be explained by the hydration reaction. After the specimens were immersed in the water, the unreacted KH_2PO_4 in the matrix was acidic in the water. Therefore, the hydration reaction in the matrix proceeded in the opposite direction. The MKP at the interface between the fibres and the matrix was reduced, so the fibre could not be completely wrapped by the matrix leading to the weak bond behaviour.

Fig. 8 shows the retention rate of the compressive strength, bond strength, and pullout energy of the specimen after the immersion in the water based on the data in Tabs. 4 and 5. Fig. 8(a) and Fig. 8(b) show that the longer immersion time caused a more obvious decline of each index. In addition, it is found that the bond behaviour is more sensitive to the influence of the water than the compressive strength.


(a) 7 days

(b) 28 days

Figure 8: Retention rate of compressive strength, average bond strength and pullout energy at different immersion age

As the M/P increased, the retention rate of the matrix compressive strength was improved, especially for the specimens immersed in the water for 28 days. When the M/P was 4, the specimens showed the highest compressive strength due to the abundant existence of the MKP, thus formed a skeleton structure with the unreacted magnesium oxide. The strength retention rate is the highest when immersed for 7 days.

The maximum retention rate of the bond strength was found at M/P=4, which was slightly larger than other groups (M/P=3, 5, 6). This may be due to the higher compressive strength of the cement matrix before the immersion leading to higher initial bond strength. The sufficient bond strength protected the interface from the corrosion of the water. Therefore, the specimens with M/P of 4 performed better bond behaviour.

3.2.4 SEM analysis

The micro-morphology of the interface zone between steel fibre and MPC matrix was analysed using a scanning electron microscope (SEM). The SEM photos of the interface zone with M/P of 3, 4, 5 and 6 are shown in Fig. 9, Fig. 10, Fig. 11 and Fig. 12, respectively.
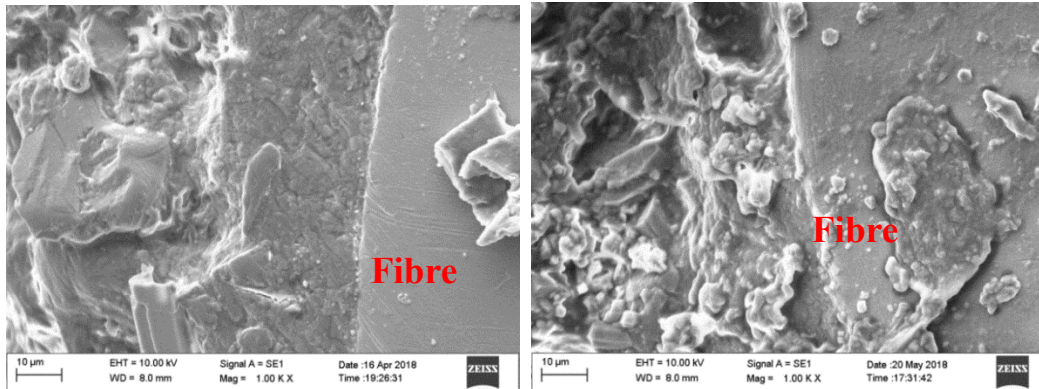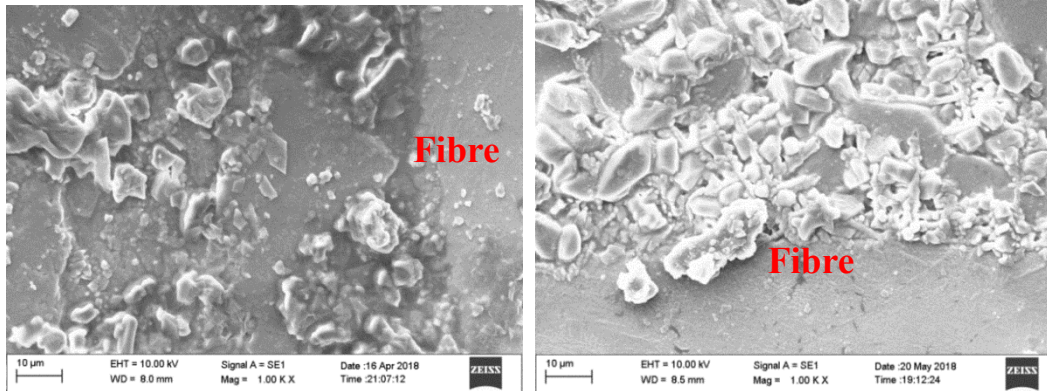
(a) Interface zone without immersion into water   (b) Interface zone immersed into water for 28 days

Figure 9: Micromorphology of the interface zone between the steel fibre and matrix prepared with MPC of M/P=3
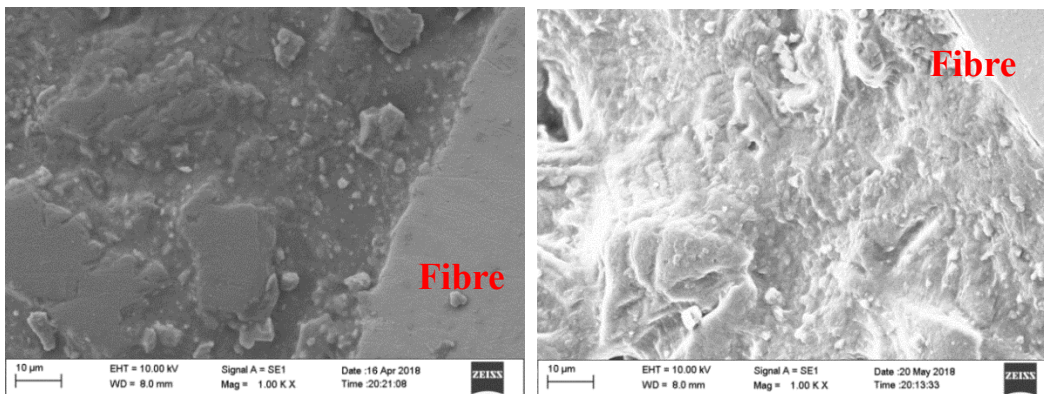
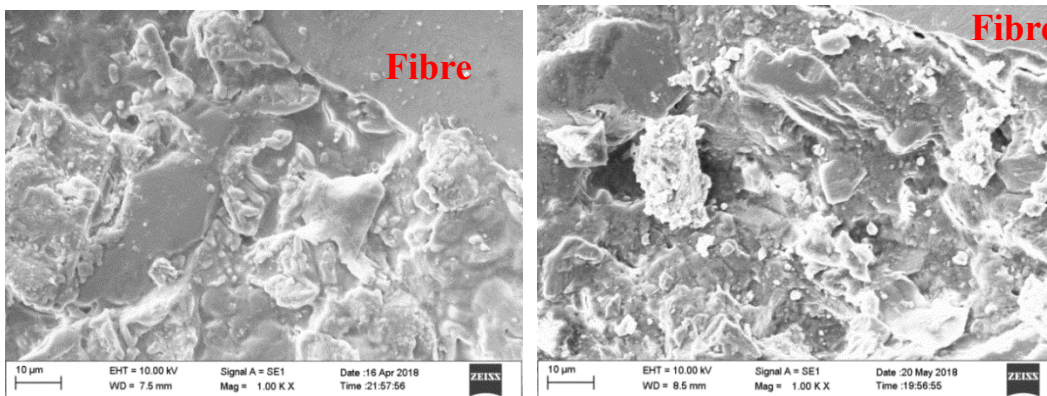(a) Interface zone without immersion into water   (b) Interface zone immersed into water for 28 days

Figure 10: Micromorphology of the interface zone between the steel fibre and matrix prepared with MPC of M/P=4

(a) Interface zone without immersion into water   (b) Interface zone immersed into water for 28 days

Figure 11: Micromorphology of the interface zone between the steel fibre and matrix prepared with MPC of M/P=5

(a) Interface zone without immersion into water   (b) Interface zone immersed into water for 28 days

Figure 12: Micromorphology of the interface zone between the steel fibre and matrix prepared with MPC of M/P=6

Fig. 9(a), Fig. 10(a), Fig. 11(a) and Fig. 12(a) present the micro-morphology of the interface zone without immersing into water. For the interface zone without immersing into water, the compaction of the interface zone with M/P of 4 was the highest. Some unreacted potassium dihydrogen phosphate was found in the interface zone with M/P of 3. Excessive MgO was found in the interface zone with M/P of 5 and 6. For the compaction of the interface zone between the steel fibre and MPC matrix, the most appropriate M/P was 4.

Fig. 9(b), Fig. 10(b), Fig. 11(b) and Fig. 12(b) present the micro-morphology of the interface zone immersing into water for 28 days. After the samples were immersed in water for 28 days, the hydration product MKP in the interface zone with different M/P was significantly reduced and the compaction of the interface zone was weakened. The degradation mechanism of the interface immersed in water was similar to that of the MPC-matrix immersed in water. The unreacted potassium dihydrogen phosphate

(KH_2PO_4) in the interface was dissolved leading to the acidic aqueous solution. Then the reaction proceeded in the opposite direction and the content of MKP was reduced. Due to the unreacted potassium dihydrogen phosphate, the compaction of the interface zone with M/P of 3 was weakened most seriously after immersing in water. However, some unreacted potassium dihydrogen phosphate was found in the interface with M/P of 4, 5 and 6. The water stability of the interface with M/P of 4, 5 and 6 was higher than that of the interface with M/P of 3. Additionally, the compaction of the interface zone with M/P of 4 was the highest. It can be observed that the permeability of the interface zone with M/P of 4 was the lowest. The least water penetration occurred into the interface with M/P of 4. Therefore, the interface zone between the steel fibre and MPC-matrix with M/P of 4 presented the best water stability.

4 Conclusions

A series of pullout tests of steel fibres embedded in the MPC-based matrix were carried out. The parameters investigated in this experimental study included the composition of the MPC matrix and the immersion age of the specimens. Based on the experimental results, the average bond strength and the pullout energy were investigated. The influence of water on the microscopic characteristics of the interface transition zone was also analyzed by using scanning electron microscope (SEM). The following conclusions can be drawn based on the experimental results presented in this study.

(1) The compressive strength of MPC based mortar decrease significantly with the increase of the immersion time in water. The compressive strength of the MPC based matrix decreased by more than 30% when the specimens were immersed in the water for 28 days.

(2) The retention rate of the compressive strength of MPC mortar increase significantly with the increase of the MgO-KH_2PO_4 mole ratio (M/P) of the MPC from 3 to 6. The increase of the magnesia in the MPC significantly improved the water stability of MPC composites.

(3) The bond performance between the steel fibre and the MPC based matrix degrade significantly with the increase of the immersion time in water. The effect of the water on the interface between the steel fibre and the MPC-matrix was found to be more significant compared to the composition of the MPC-matrix. The average bond strength between the steel fibre and the MPC based matrix decreased by more than 50% when the specimens were immersed in the water for 28 days.

(4) An appropriate M/P of the MPC improves the water stability of the interface zone between the steel fibre and MPC-matrix. The interface zone between the steel fibre and MPC-matrix with M/P of 4 possessed the best water stability in this study.

References

CS (Chinese Standard) GB/T 17671-1999, Cement mortar strength testing method (ISO) (In Chinese).

CS (Chinese Standard) CECS 13:2009, Standard test methods for fiber reinforced concrete (In Chinese).

Ding, Z. (2005): *Research of magnesium phosphosilicate cement*. Hongkong University of Science and Technology.

Ding, Z.; Dong, B.; Xing, F.; Han, N.; Li, Z. (2012): Cementing mechanism of potassium phosphate-based magnesium phosphate cement. *Ceramics International*, Vol. 38(8), pp. 6281-6288.

Frantzis, P.; Baggott, R. (2003): Transition points in steel fibre pull-out tests from magnesium phosphate and accelerated calcium aluminate binders. *Cement & Concrete Composites*, vol. 25, no. 1, pp. 11-17.

Frantzis, P.; Baggott, R. (2000): Bond between reinforcing steel fibres and magnesium phosphate/calcium aluminate binders. *Cement & Concrete Composites*, vol. 22, no. 3, pp. 187-192.

Feng, H.; Sheikh, M. N.; Hadi, M. N. S.; Gao, D. Y.; Zhao, J. (2018): Mechanical properties of micro-steel fibre reinforced magnesium potassium phosphate cement composite. *Construction and Building Materials*, vol. 185, pp. 423-435.

Feng, H.; Chen, G.; Gao, D. Y.; Zhao, K.; Zhang, C. (2018): Mechanical properties of steel fiber-reinforced magnesium phosphate cement mortar. *Advances in Civil Engineering*, pp. 1-11.

Feng, H.; Sheikh, M. N.; Hadi, M. N. S.; Feng, L.; Gao, D. Y. et al. (2018): Interface bond performance of steel fibre embedded in magnesium phosphate cementitious composite. *Construction and Building Materials*, vol. 185, pp. 648-660.

Gao, R. (2014): Study on properties of modified magnesium phosphate cement-based materials. *Xi'an University of Architecture and Technology*.

Meng, W.; Deng, Y. F.; Sun, Q. (2014): Effect of steel fiber on mechanical properties of polymer cement mortar. *Journal of Huaihai Institute of Technology (Natural Science Edition)*, vol. 1, pp. 50-53.

Pera, J.; Ambroise, J. (1998): Fiber-reinforced magnesia-phosphate cement composites. *Cement & Concrete Composites*, vol. 2, no. 20, pp. 31-39.

Shannag, M. J.; Brincker, R.; Hansen, W. (1999): Pullout behavior of steel fibers from cement-based composites. *Cement & Concrete Research*, vol. 27, no. 6, pp. 925-936.

Soudée, E.; Péra, J. (2002): Influence of magnesia surface on the setting time of magnesia-phosphate cement. *Cement & Concrete Research*, vol. 32, no. 1, pp. 153-157.

Wang, H. T.; Qian, J. S.; Cao, J. H.; Shen, B. (2006): Properties and application of steel fiber reinforced magnesium phosphate cement mortar. *Construction Technology*, vol. 37, no. 6, pp. 462-464.

Wille, K.; Naaman, A. E. (2012): Pullout behavior of high-strength steel fibers embedded in ultra-high-performance concrete. *ACI Materials Journal*, vol. 109, no. 4, pp. 479-488.

Xiao, W. (2015): Physical and mechanical properties and durability of rapid repair materials for magnesium phosphate cement airport. *Nanjing University of Aeronautics and Astronautics*.

Yan, Y. L. (2010): Experimental research and engineering application of new early strength magnesium phosphate cement. *Shanghai Jiaotong University*.

Yang, Q.; Zhu, B.; Wu, X. (2000): Characteristics and durability test of magnesium phosphate cement-based material for rapid repair of concrete. *Materials & Structures*, vol. 33, no. 4, pp. 229-234

Yang, Q.; Wu, X. (1999): Factors influencing properties of phosphate cement-based binder for rapid repair of concrete. *Cement & Concrete Research*, vol. 29, no. 3, pp. 389-396.

Yang, N. (2014): *Study on the Bonding Properties of Magnesium Phosphate Cement Based Materials*. Hunan University.

Yang, Q. B.; Wu, X. L. (1999): Research on new ultra-fast hard phosphate repair materials. *Concrete and Cement Products*, vol. 6, pp. 13-15.

Zhao, K. P. (2017): *Mechanical Properties and Overlay Repair Test of Fine Steel Fiber Magnesium Phosphate Cement Mortar*. Zhengzhou University.